7

Semiconducting Polymer-based Bulk Heterojunction Solar Cells

Matthew Schuette White and Niyazi Serdar Sariciftci

Linz Institute for Organic Solar Cells, Institute for Physical Chemistry, Johannes Kepler University, Linz, Austria

Abstract

This chapter serves as an introduction to polymer-based solar cells. The fundamental processes involved in converting sunlight into electrical power by semiconducting polymers are described. This includes the optical, electrical, and mechanical properties of polymers that are either beneficial or detrimental for solar cell design and fabrication. The methods for processing polymer solar cells and state-of-the-art efficiencies and cell lifetimes are reviewed.

Keywords: Polymer solar cells, organic photovoltaics, bulk-heterojunction

7.1 Introduction

Polymer based bulk heterojunction (BHJ) solar cells are the subject of much academic and industrial interest [1–3, 19]. In 1992, Sariciftci *et al.* first demonstrated photo-induced electron transfer from a polymer to C_{60} [4]. This breakthrough allowed semiconducting polymers to be used as donors in heterojunction solar cells [5]. Such a system consists of a semiconducting polymer acting as an electron donor (D) and a fullerene acting as an acceptor (A). Though both the D and A components may absorb light, the polymer generally is the principle contributor. Photo-excitation in semiconducting polymers does not result in delocalized free carriers, as in conventional semiconductors. Rather it creates bound electron-hole pairs known

Vikas Mittal (ed.) Polymers for Energy Storage and Conversion, (199–214)

as excitons that must diffuse to the D-A interface where they dissociate, resulting in D^+ - A^-. The charges may then be conducted through the respective D and A phases to the cathode and anode resulting in photocurrent.

A limiting factor in constructing an efficient photovoltaic device from such a system is the exciton diffusion process. Excitons can diffuse roughly 10 nm, which dictates the distance from a D-A interface where absorbed photons can contribute to the photocurrent. For a planar interface, there is simply insufficient volume within 10 nm to generate significant power. Thus, a BHJ is required with a 3 dimensional D-A morphology and phase separation on the 10 nm scale. A bicontinuous network of the two phases is required to efficiently extract the charges.

The challenges in generating real photovoltaic cells from semiconducting polymers are numerous, but can be summarized as follows. Absorb as much light as possible spanning the solar spectrum. Form an ideal nano-morphology to maximize exciton dissociation but allow efficient charge extraction. Minimize energy losses through recombination and parasitic resistances. Eliminate reactive components that will limit device lifetimes. And finally, exploit the advantages of polymer semiconductors to their fullest.

Polymers bring with them a variety of desirable (and some undesirable) properties which factor into their use for solar power, whether for niche applications or for large scale harvesting. This chapter will provide an overview of these properties.

7.2 Optical Properties of Semiconducting Polymers

The very first physical process involved in the photovoltaic power conversion is the absorption of light in a semiconductor [17, 19]. Photons are absorbed in semiconducting polymers resulting in distortions of the local electronic structure. The simplest conjugated polymer is polyacetylene. This chain of sp^2p_z hybridized carbon atoms is the backbone for all conjugated polymers. Here, each of the N carbon atoms each contribute one p_z-electron. Yet each state in the π-band can accommodate two electrons, one of each spin. To first order, the π-band could be considered a continuum of states that is exactly half filled, resulting in a metallic polymer. This situation requires that the bond length is uniform along the chain, which is

not the case in reality. The lower energy configuration entails alternating weaker and stronger π-π bonds. This results in slightly longer single bonds (1.45 Å) and shorter double bonds (1.35 Å) alternating along the conjugated backbone. This is a result of the Peierls instability and causes an energy gap to form at the Fermi energy, known as the Peierls gap. In polyacetylene, flipping all of the double bonds results in a configuration of equal energy. The bandgap (~1.8 eV) corresponds to the energy required to locally reconfigure the bonds.

Primary photexcitations in semiconducting polymers are the subject of much ongoing discussion, but we will begin with a molecular spectroscopy perspective. The absorption of a photon with sufficient energy results in the population of the first excited state (S_1) and the depopulation of the ground state (S_0). The polymers are essentially molecular solids and the first order description of the optical transitions can be considered as such. Each electronic state (S_0, S_1, etc.) can be approximated by a molecular potential energy surface. For each electronic state there are associated vibrational levels (v_0, v_1, etc.) associated with the nuclear coordinates. The absorption profile of a molecular chromophore comprises the transitions from the ground state (S_0v_0) to the vibrational levels in the S_1 state. The relative intensities of these vibronic transitions depends on the overlap integral of the wave function of the initial and final states. The v_0 wavefunction is localized in the center of the potential, but the higher order vibrational levels are concentrated near the potential energy surface at the classical turning points. These energy levels and associated transitions are outlined in Figure 7.1a. The resulting absorption spectrum for a molecular chromophore is shown in Figure 7.1b. However, typical semiconducting polymers do not show such sharp features in absorption. The polymers are molecular solids where the localized chromophores experience various physical conditions, and the resulting bond lengths are not identical. Therefore, the polymer absorption spectrum is characterized by broad vibronic peaks that smear out the absorption profile as seen in Figure 7.1c. This smooth, broad-band absorption is advantageous for photovoltaics.

The electronic transitions in conjugated polymers are $\pi \rightarrow \pi^*$ transitions that are spin and orbital allowed, and therefore have very strong extinction coefficient. For example, the common polymer fullerene blend of P3HT:PCBM, has absorption coefficient of over 5×10^{-4} cm^{-1} for photon energies between 2.2 and 3 eV. This means that over 68%

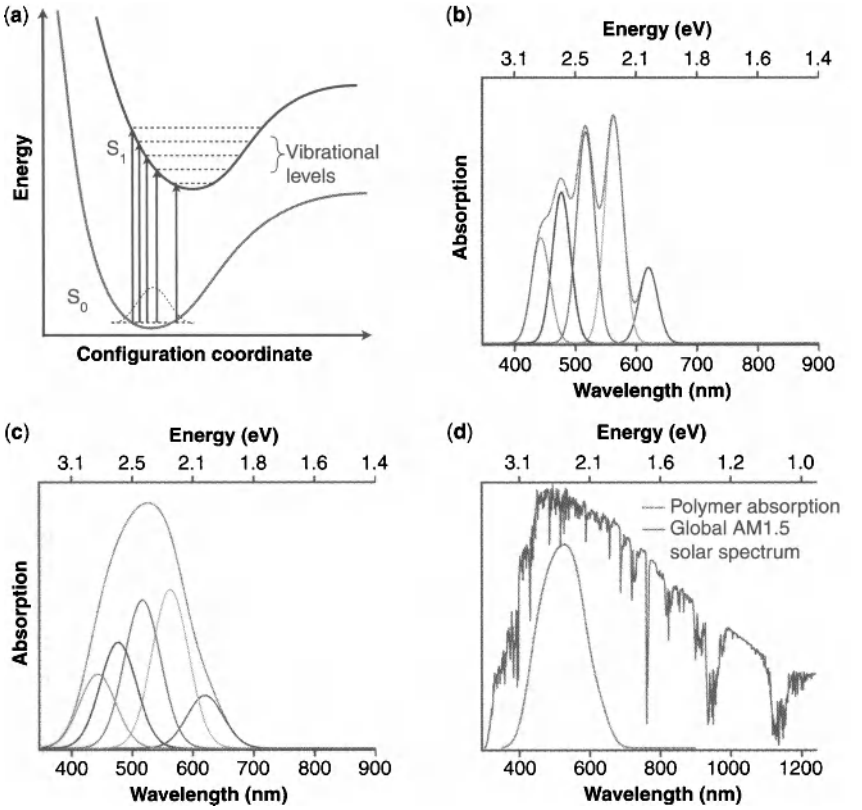

Figure 7.1 (a) Schematic showing the electronic energy levels S_0 and S_1, and the vibrational levels in S_1. Vibronic transitions occur upon absorption of light, resulting in vertical transitions from the lowest vibrational state of S_0 to any of the vibrational states of S_1. The relative intensities of the transitions are determined by the overlap of the wave functions. (b) An example of a molecular absorption spectrum, with well defined vibronic peaks. (c) A polymer film shows positional and energetic disorder, resulting in a smeared-out absorption spectrum. (d) Comparison of the example polymer absorption spectrum with the incident solar spectrum. Optimizing the overlap is key for photovoltaics.

of the incident light in that spectral range is absorbed in a film of only 100 nm. The transition moment, along the carbon-carbon double bond axis, is randomly oriented throughout a polymer solid and so most organic semiconductors are anisotropic. Semiconducting polymers generally are very good at absorbing light, which relaxes constraints when designing photovoltaic devices.

The principle challenge in designing semiconducting polymers is not to increase the absorption coefficient, but to optimize the

overlap of the polymer absorption spectrum with the incident solar spectrum. As seen in Figure 7.1d, the absorption of the generic polymer from Fig 1c does not overlap particularly well with the AM1.5 global spectrum. Reducing the bandgap of the polymer shifts the absorption edge to lower energy and longer wavelength. There are several methods to accomplish this bandgap reduction, and several corresponding methods to absorb the higher energy light that may fall outside the absorption of a low bandgap polymer [6, 7].

The logical first approach to reduce the bandgap of a semiconducting polymer is to minimize the bond-length alternation. By reducing the Peierls gap, the material becomes more like a 1 dimensional metal complete with the small optical bandgap. Many polymer semiconductors are poly(heterocycles), of which poly(thiophene) (PT) is perhaps the most common. There are two mesomeric forms of PT, which are not energetically equivalent, shown in Figure 7.2a. The aromatic form of PT is much more favorable than the quinoid form. Consequently, the thiophene-thiophene linkages display predominantly single bond character resulting in pronounced bond length alternation. The bandgap is roughly 2 eV.

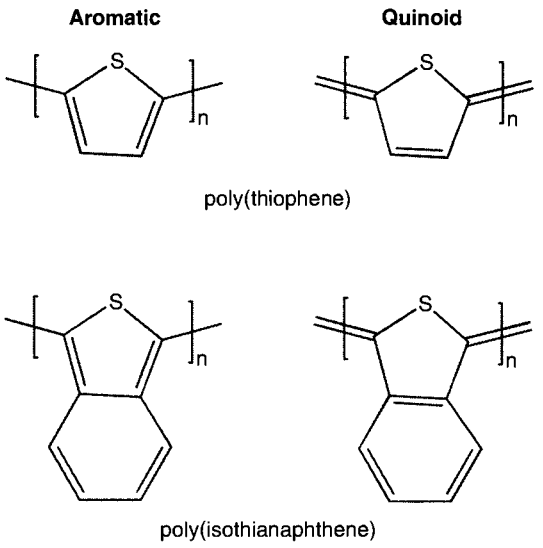

Figure 7.2 Chemical structures of (a) PT, and (b) PITN in both aromatic and quinoid forms. The quinoid form of PITN shows an increase in aromaticity of the fuzed benzene ring, resulting in a much lower bandgap.

As first demonstrated in 1984, by Wudl *et al.*, the badgap can be drastically reduced by changing the repeat unit to favor the quinoid structure [8]. There are many such polymers, but the primary example is poly(isothianaphtene) (PITN), as seen in Figure 7.2b. The quinoid mesomer PITN results in a gain in aromaticity of the fused benzene ring. This effect reduces the energetic difference between the two configurations, reduces the bond-length alternation, and results in a bandgap of ~1 eV. This is a clear example of how small changes in polymer chemical structure can drastically change the optical and electronic properties of semiconducting polymers.

Another very successful approach to increase the double-bond character between the repeat units is the push-pull approach. Here, two complementary monomers form a dimerized repeat unit for the semiconducting polymer. These alternating units are electron donating (D) and electron accepting (A). These donors and acceptors can accommodate charges which enables a mesomerism of the type ($D\text{-}A \leftrightarrow D^{+} = A^{-}$), thus increasing the double-bond character of the linkages. In such cases, there is a high degree of freedom in designing the push-pull polymer. The D-unit can be as simple as a thiophene or pyrrole heterocycles, or they can be much more complicated. The A-unit can be equally varied, though benzothiadiazole is a common example. This push-pull approach has proved highly successful and has driven the improvement of OPV efficiency from 4% in 2005 to over 9% today in a single junction polymer-fullerene BHJ. It is instrumental in the realization of tandem OPV cells with efficiency of 10.6%, for the red/near IR absorbing cell.

For a helpful example, we will look at the photophysics of an example push-pull polymer presented by Jespersen *et al.* The polymer DiO-PFDTBT consists of alternating 9,9-ethylhexyl-9 H-fluorene and 4,7-di-thiophen-2-yl-benzo[1,2,5]thiadiazole [9]. In this system the benzothiadiazole is the electron withdrawing unit and the thiophene is the donor. This system shows a characteristic "camel-back" absorption with two strong absorption peaks. The lower energy peak (in this case at 2.26 eV) is shown to be due to the charge transfer state with the electron concentrated on the benzothiadiazole unit, and the hole delocalized along thiophene and fluorine units. The higher energy (3.4 eV) is the $\pi \rightarrow \pi^{*}$ transition, exchanging the single and double bonds along the

conjugated polymer. In this particular polymer, the bandgap is roughly equivalent to P3HT and so it is not considered a low-bandgap semiconductor. However, the push-pull polymer family contains materials with bandgap lower than 0.5 eV. Recently poly(thieno[3,4-b]thiophene/benzodithiophene) (PTB7) has been used to make a single junction polymer solar cell with efficiency of 9.2% [10]. PTB7 has a bandgap of 1.6 eV and absorbs strongly between 500 nm and 750 nm. The higher energy light is absorbed by the fullerene derivative $PC_{71}BM$.

Polymers can absorb a significant portion of the solar spectrum. Once the photon has been absorbed, the ability to extract the energy from the device in a meaningful way requires the combination of several processes. The primary processes involved are vibrational relaxation, exciton diffusion, exciton dissociation, charge separation and extraction. Competing, at each step, is charge recombination which results in energy loss through either radiative or non-radiative processes.

When higher energy photons populate the higher vibrational levels, the system quickly relaxes (less than 100 fs) to the lowest vibrational level in the excited singlet state [4, 19]. This excited state electron still feels the Coulombic attraction of the hole, and the pair forms an exciton. Specifically, this is an intrachain exciton which extends over a few repeat units of the chain. The lifetime of such excitons ranges from a few to a few hundred picoseconds. Within this lifetime, the exciton must diffuse within they polymer phase of the BHJ to a location compatible with photo-induced charge transfer to the fullerene acceptor (D-A interface). Transient luminescent measurements show that the exciton migration in pristine polymers is complete within 10 ps. If the exciton does not approach a D-A interface within it's lifetime, it will recombine and the energy is lost via fluorescence. If, however, the exciton is in the presence of a D-A interface, ultrafast (< 100 fs) electron transfer occurs via $D^* + A \rightarrow D^+ + A^-$. The reverse process, the recombination of the geminate pair, occurs at the μs scale at room temperature. Only the combination of ultrafast electron transfer and slow electron-hole recombination in the D-A system allows for harvesting of the photon energy in BHJ solar cells.

The exciton diffusion occurs over a timescale of roughly 10 ps, and over length-scale of roughly 10 nm. These have been measured

independently by transient photoluminescence, spectrally resolved photoluminescence in bilayers, and by acceptor concentration variance in BHJ blends. These values of course vary in different polymers and even in different packing configurations of the same polymer. But it should be noted that the diffusion length corresponds roughly to the product of the exciton decay lifetime with the speed of sound in the polymer host.

This exciton diffusion length is what determines the optimum phase dimensions within a BHJ blend. Controlling this phase separation at the 10 nm scale requires good control through self-assembly. The relative solubility of the two materials in the processing solvent is a primary factor. Processing additives can be used to further optimize the separation, a technique that has seen great success. Thermal annealing also results in phase separation and can be controlled through temperature, time, and by selecting materials with compatible glass transition temperature.

Once the electron is transferred to the acceptor phase, it is not entirely clear by which process the electron and hole are separated to overcome their inherent Coulombic attraction. It has been proposed that delocalization of the electron in a fullerene acceptor phase is sufficient. It has also been proposed that the excess energy resulting from the LUMO-LUMO offset is converted to kinetic energy allowing for escaping the Coulomb potential. Further complicating the issue, it appears that a larger offset energy does not translate into more efficient free charge generation. One must balance the change in Gibbs free energy with the reorganization energy of the polymer upon charge transfer. This particular process is still the subject of much investigation and debate.

7.3 Electrical Properties of Semiconducting Polymers

Following the generation of free carriers, they must be transported through their respective phases to the electrodes [11, 18, 19]. Therefore, the carrier mobility of electrons in the acceptor phase and holes in the donor phase are critical material properties. The product of the mobility and the field strength determines the carrier velocity. The limiting thickness of the polymer solar cell is approximately the product of this velocity with the recombination

lifetime. The effective carrier mobility of electrons and holes in the bulk must also be matched, but this can be further tuned by morphology of the two phases.

In semiconducting polymers, positional and energetic disorder results in a breakdown of the band transport model. The carrier wave-functions are localized and k no longer functions as a good quantum number. Therefore, transport is governed by hopping processes. In such a system, the lowest energy states, so called "tail states" are localized and the higher energy states are more delocalized resulting in higher mobility. Therefore, overall mobility in polymer semiconductors is heavily dependent on temperature, carrier concentration, as well as electric field. The mobility increases with temperature due to higher thermal activation of carriers from the tail states. This is the opposite temperature dependence from metals and conventional semiconductors, where conductivity increases at lower temperature. The carrier concentration dependence arises from populating the tail states allowing additional carriers to fill the high mobility band states. The field dependence tends to follow a Poole-Frenkel behavior, reflecting the lowered activation energy from a localized state in the presence of an external electric field. This generally results in an increased mobility under stronger fields. However, there have been demonstrations of the reverse effect, thought to result from spatial disorder in a BHJ blend. Because the transport in such a blend requires some random-walk behavior, high field strength is believed to trap a fraction of carriers in "dead-ends", effectively reducing the number of potential pathways.

The carrier mobility in the semiconducting polymers does limit the overall thickness of the solar cell. For example, we can approximate the limiting thickness as $L \approx (\mu V \tau)^{1/2}$, where V is the driving potential and τ is the carrier lifetime. In Figure 7.3 we plot an example with $\tau = 1$ μs, for various V. Here, a polymer with $\mu = 10^{-3}$ cm^2/Vs will allow for a solar cell on the order of 100 nm thickness. This value varies by a factor of $\sqrt{10} = 3.16$ for every order of magnitude increase of either μ or τ. Reasonable estimates for τ range between 1 and 10 μs and many semiconducting polymers have shown carrier mobility between 10^{-4} and 10^{-3} cm^2/Vs. Therefore, most BHJ films are on the order of 100 nm thick. Given the strong light absorbing properties of the polymers discussed in the previous section, this is generally sufficient to absorb most of the incident light. However, some polymers are mobility limited and can only be used in layers

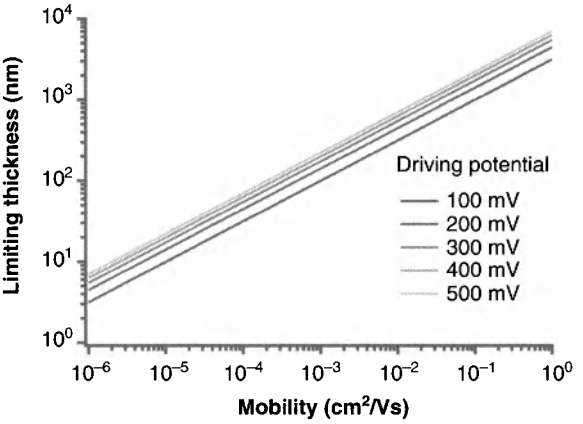

Figure 7.3 Estimated thickness limit for a BHJ layer as a function of carrier mobility. Most semiconducting polymers limit the film thickness to roughly 100 nm.

of 80 nm or below. This includes old research standards of PPV, and new low bandgap polymers that nonetheless result in high efficiency. Still other polymers have high carrier mobility ($>10^{-3}$ cm^2/Vs), and can yield perfectly functional devices with thickness over 500 nm. This may be excessive thickness for optical absorption, but thicker layers are easier to process rapidly and reproducibly.

7.4 Mechanical Properties Polymer Solar Cells

Polymer solar cells do not offer many advantages over conventional solar cells in terms of efficiency or lifetime. There is a potential cost advantage, gained largely through the processing methods described above. But polymer solar cells do have several mechanical properties where they excel as no other technology can. Principle among these are the low weight and high flexibility of the films. These two advantages are directly linked to the fact that polymer solar cells are extremely thin, on the order of 300 nm.

Light-weight power sources are applicable for aviation, space, and remote personal use, among other applications. They may be applied, unobtrusively, directly to the surface of a desired object, or simply carried along for lower pay-load. Any person who must carry their power supply with them into remote regions would

benefit from weight reduction. This includes military personnel, research expeditions, and personal adventurers.

Flexible solar cells are easier to pack into smaller spaces, are less susceptible to physical damage, and can be integrated into moving parts for robotics or other applications. Direct integration into clothing or even onto human skin could potentially power smart medical devices (bandages etc.) or clothing. These future technologies would place very specific requirements on the flexibility of the solar cells. Namely, the devices must withstand bending to radius significantly less than 1 mm, in order to survive the creasing and flexing that standard clothing and bandages are subjected to.

Typical flexible plastic substrates are roughly 100 μm thick, roughly 200 times thicker than the active components of a polymer solar cell. Consequently, the flexibility and weight are entirely determined by the substrate. Such a flexible device can only be bent to a radius of roughly 1 cm if there is a brittle ITO electrode. Radius of curvature ≤5 mm can be obtained if ITO free polymer or carbon-nanotube network electrodes are used [12].

Very recently plastic substrates only 1.4 μm thick were used to fabricate fully functional OPV devices [13]. Combined with roughly 500 nm of electrodes (PEDOT:PSS, and Ca/Ag), and active layer (P3HT:PCBM), they are less than 2 μm in total. This is thinner than a thread of spider silk, but can be extremely large in area. The foil is a commodity scale roll-to-roll processed Mylar used for foil capacitors. In total, they weigh only 4 g/m^2. Even with modest polymer OPV efficiency of 4.2%, this results in a record specific weight of 10 W/g. Organic PV is therefore the leading candidate when weight is an issue, so long as device lifetimes are acceptable. Combining ultrathin substrates with more air-stable electrodes would be necessary before any such film could be commercially available.

Furthermore, these ultrathin devices are shown to be flexible with radius of curvature under 10 μm. As an example, the solar cells are shown wrapped around a human hair of radius ~35 μm, in Figure 7.4a. They can literally be crumpled like a tissue under continuous operation. Flexibility to such a degree allows the devices to be adhered directly onto an elastomer, and subjected to 400% tensile strain. The strain is accommodated by the formation of a random network of wrinkles and folds, as seen in Figure 7.4b. This demonstrates compatibility with malleable surfaces such as human skin.

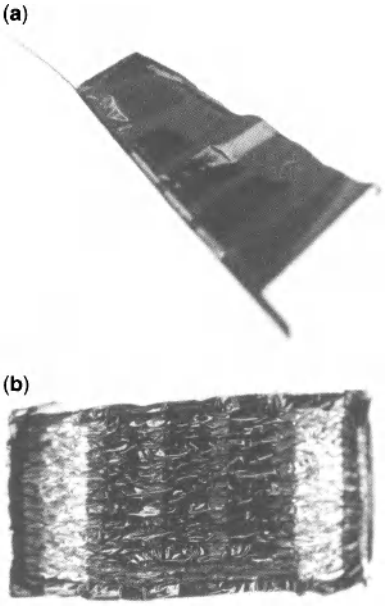

Figure 7.4 (a) An ultrathin polymer solar cell wrapped around a human hair of radius ~ 35 μm. (b) An ultrathin polymer solar cell compressed on the surface of an adhesive elastomer, forming a random network of wrinkles and folds.

7.5 Processing of Polymers

One of the key advantages of polymers, when considering both the cost and the scalability of manufacturing, is that they are compatible with solution processing [14]. Therefore, any painting or printing technology can be used to deposit semiconducting polymers. When combined with flexible polymer based substrates, these enable the use of roll-to-roll processing. In order for any photovoltaic technology to meet the terawatt challenge, extremely high throughput manufacturing techniques must be employed. Assuming reasonable efficiency and lifetime of the panels, one can estimate that at least 3 standard football fields of PV area must be manufactured every minute simply to account for the panels dying at the end of their life cycle. Therefore, compatibility with high throughput roll-to-roll processing is critical.

Simple laboratory solution processes include spin-coating and doctor blading. These can be used very efficiently for processing up to a few 10's of cm linear dimension substrates. They are ideal for laboratory use on small scales and for low throughput. Doctor blading involves dragging a flat metal edge at a controlled velocity

directly above the surface of the substrate. The polymer semiconductor solution is dispersed along the gap between the blade and the substrate. From a laboratory standard, it produces very homogeneous, relatively large area films using comparatively little material.

The roll-to-roll analogue of doctor blading is knife-coating. Here, the blade is stationary but the substrate moves underneath it in the process line. And similarly to doctor blading, the ink is dropped onto the substrate prior to contact with the blade. A similar technique injects the ink through a slot in the blade itself. This is known as slot-dye coating and is schematically shown in Figure 7.5a. It results in similarly homogeneous films but presents one distinct advantage

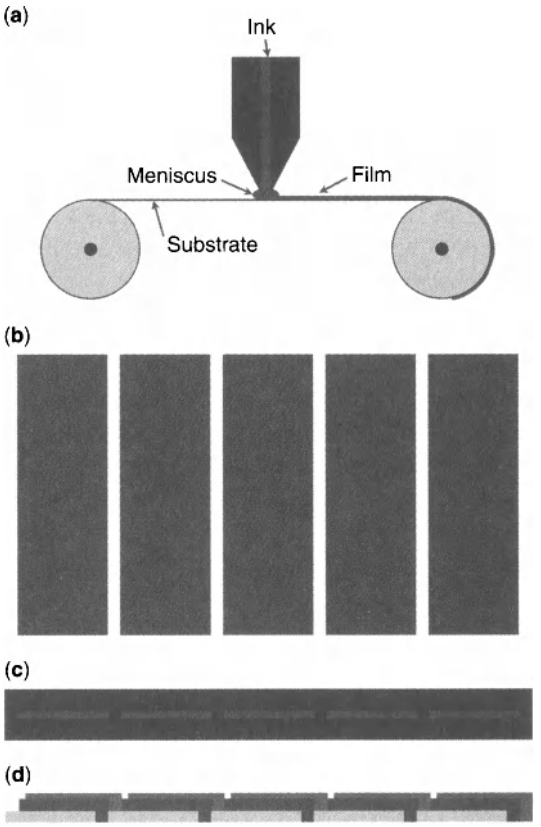

Figure 7.5 Schematic of slot-die coating for polymer solar cell modules. (a) Cross sectional view of a roll-to-roll slot die coater. (b) Typical "parallel stripe" pattern for roll-to-roll produced polymer solar cell module. (c) One dimensional patterning in a slot-die coater, top-down view. d) Cross sectional view of a serial-connected module, coated in the parallel stripe pattern.

over all other high-throughput techniques. The ink inlets can be patterned along the length of the blade (Figure 7.5c), resulting in uniform pattern of stripes on the substrate. This parallel stripe cell pattern, shown in Figure 7.5b, is very common for OPV modules. By overlapping consecutive electrode layers (Figure 7.5d), a series connection between the cells allows for rapid module construction. Slot dye coating has lateral resolution of roughly 100 μm, so unused space can be minimized. It is considered the best technique for printing polymer based solar cells.

Several other techniques are also applicable, though they have drawbacks with respect to either processing speed or patterning accuracy. Ink-jet printing is a very interesting method for fabrication of organic electronics, with potential custom printing advantages. It offers very good resolution and the capability of printing multiple functional inks in different patterns. It is not, however, a high throughput method. Screen printing may also be used to pattern polymer inks, and offers higher throughput than ink-jet printing, but is not applicable for uniform films on the 100 nm thickness scale. Air-brush and conventional paint-brush techniques may also be used, though film uniformity becomes an issue.

Recent advances have allowed for polymer based tandem OPV devices with complementary optical absorption and current matching. This cell design presents a further processing challenge. Construction of one cell on top of the other may dissolve the already dry layers. Fortunately, sequential layers can be processed from orthogonal solvents. PEDOT:PSS, for example, is dispersed in water and can be blended with DMSO, or a variety of alcohols for processing. It does not dissolve in the non-polar solvents often used for processing of the semiconducting polymers such as chloroform, chlorobenzene, or toluene. The opposite is also true, where the semiconducting polymers do not dissolve in the water/alcohol solvents for a subsequent PEDOT:PSS layer. Therefore, they can be sequentially applied so long as each step uses an orthogonal solvent to the step prior.

7.6 State-of-the-art of the Technology

The current efficiency record for a single-junction cell base on polymer semiconductor is 9.2% [10]. This cell takes advantage of a low band-gap polymer, a light absorbing fullerene, and an electron donating, surface modifying polymer for increased air stability.

Such surface modifying interlayers, including both polymers and oxides, are critical for air-stability of the solar cells as they eliminate the need for low work-function metal electrodes.

Tandem cell geometries offer the potential to surpass single junction polymer BHJ devices. Currently, a tandem geometry (exact structure is unpublished at the time of writing) holds the efficiency record for polymer based photovoltaics at 10.6% [3, 15]. This is achieved by current matching in two complementary cells in series, resulting in an addition of the driving voltages.

The lifetime of state-of-the-art polymer solar cells is equally impressive [16]. Standardized measurements of OPV lifetime have improved due to consensus procedures from the International Summit on OPV Stability. Many flexible cells and sub-modules are reported to have T_{80} lifetimes between 5 to 7 years. The lower lying energy levels of the low-bandgap polymers tend to be inherently more air-stable. Combined with air-stable electrodes and interlayers, and advances in encapsulation and packaging, these values have been growing rapidly.

The technology is has exceeded the symbolic milestone of 10% efficiency and is approaching 10 year lifetime. The technology is compatible with high throughput roll-to-roll processing, demonstrated by several test lines and even a partially functioning manufacturing facility. OPV thin film solar cells are extremely light weight, delivering more peak power per unit weight than any other solar technology. They are inherently flexible and, when constructed on ultrathin substrates, can be bent to a 10 μm radius of curvature. This is roughly equivalent to a dull razor blade. Future progress cannot be predicted with any certainty, but the trends for all metrics regarding polymer solar cells are highly promising. Whether the technology evolves into a commercially viable product remains to be seen, but the results of intense research efforts have proven that the lofty ideals of light weight, flexible, efficient, long-lived polymer solar cells are very real. There is no other photovoltaic technology on par in terms of weight, flexibility, and processing, and OPV is rapidly approaching all other technologies in terms of efficiency and device lifetime.

References

1. H. Hoppe and N. S. Sariciftci, "Organic solar cells: An overview," *J Mater. Res*, vol. 19, no. 7, pp. 1924–1945, 2004.
2. K. Coakley and M. Mcgehee, "Conjugated polymer photovoltaic cells," *Chem Mater*, vol. 16, no. 23, pp. 4533–4542, 2004.
3. G. Li, R. Zhu, and Y. Yang, "Polymer solar cells," pp. 1–9, Feb. 2012.

4. N. Sariciftci, L. Smilowitz, A. Heeger, and F. Wudl, "Photoinduced electron-transfer from a conducting polymer to buckminsterfullerene," *Science*, vol. 258, no. 5087, pp. 1474–1476, 1992.
5. G. Yu, J. GAO, J. Hummelen, F. Wudl, and A. Heeger, "Polymer photovoltaic cells - enhanced efficiencies via a network of internal donor-acceptor heterojunctions," *Science*, vol. 270, no. 5243, pp. 1789–1791, 1995.
6. J. Roncali, "Molecular Engineering of the Band Gap of π-Conjugated Systems: Facing Technological Applications," *Macromol. Rapid Commun.*, vol. 28, no. 17, pp. 1761–1775, Sep. 2007.
7. H. A. M. Mullekom, J. Vekemans, E. E. Havinga, and E. W. Meijer, "Developments in the chemistry and band gap engineering of donor-acceptor substituted conjugated polymers," *Mat Sci Eng R*, vol. 32, no. 1, p. 1, 2001.
8. F. Wudl, M. Kobayashi, and A. J. Heeger, "Poly(isothianaphthene) - The Journal of Organic Chemistry (ACS Publications)," *The Journal of Organic ...*, 1984.
9. K. G. Jespersen, W. J. D. Beenken, Y. Zaushitsyn, A. Yartsev, M. Andersson, T. Pullerits, and V. Sundström, "The electronic states of polyfluorene copolymers with alternating donor-acceptor units," *J Chem Phys*, vol. 121, no. 24, p. 12613, 2004.
10 Z. He, C. Zhong, S. Su, M. Xu, H. Wu, and Y. Cao, "Enhanced power-conversion efficiency in polymer solar cells using an inverted device structure," *Nature Photon*, pp. 1–5, Aug. 2012.
11 B. Gregg, S. Chen, and R. Cormier, "Coulomb forces and doping in organic semiconductors," *Chem Mater*, vol. 16, no. 23, pp. 4586–4599, 2004.
12 M. W. Rowell, M. A. Topinka, M. D. Mcgehee, H.-J. Prall, G. Dennler, N. S. Sariciftci, L. Hu, and G. Gruner, "Organic solar cells with carbon nanotube network electrodes," *Appl. Phys. Lett.*, vol. 88, no. 23, p. 233506, 2006.
13 M. Kaltenbrunner, M. S. White, E. D. Glowacki, T. Sekitani, T. Someya, N. S. Sariciftci, and S. Bauer, "Ultrathin and lightweight organic solar cells with high flexibility," *Nat Commun*, vol. 3, p. 770, 2012.
14 R. Søndergaard, M. Hösel, D. Angmo, T. T. Larsen-Olsen, and F. C. Krebs, "Roll-to-roll fabrication of polymer solar cells," *Materials Today*, vol. 15, no. 1, pp. 36–49, 2012.
15 M. A. Green, K. Emery, Y. Hishikawa, W. Warta, and E. D. Dunlop, "Solar cell efficiency tables (version 40)," *Prog. Photovolt: Res. Appl.*, vol. 20, no. 5, pp. 606–614, Jul. 2012.
16 M. Jorgensen, K. Norrman, S. A. Gevorgyan, T. Tromholt, B. Andreasen, and F. C. Krebs, "Stability of Polymer Solar Cells," *Adv. Mater.*, vol. 24, no. 5, pp. 580–612, 2012.
17 L. Rothberg, *Photophysics of Conjugated Polymers*, In G. Hadziioannou, and G. G. Balliaras (Eds.), *Semiconducting Polymers* (179), Weinheim, Germany, Wiley-VCH (2007)
18 V. I. Arkhipov, I. I. Fischuk, A. Kadaschuk, H. Bässler, *Charge Transport in Neat and Doped Random Organic Semiconductors*, In G. Hadziioannou, and G. G. Balliaras (Eds.), *Semiconducting Polymers* (275), Weinheim, Germany, Wiley-VCH (2007)
19 A. J. Heeger, N. S. Sariciftci, E. B. Namdas, *Semiconducting and Metallic Polymers*, Oxford, Oxford University Press (2010)